Near-Wall Modeling of the Dissipation Rate Equation

R. M. C. So* and H. S. Zhang†
Arizona State University, Tempe, Arizona 85287
and
C. G. Speziale‡
NASA Langley Research Center, Hampton, Virginia 23665

Near-wall modeling of the dissipation rate equation is investigated and its asymptotic behavior is studied in detail using a k-ε model. It is found that all existing modeled dissipation rate equations predict an incorrect behavior for the dissipation rate near a wall. An improvement is proposed and the resulting near-wall dissipation rate distribution is found to be similar to that given by numerical simulation data. To further validate the improved k-ε model, it is used to calculate flat-plate turbulent boundary-layer flows at high- as well as low-turbulence Reynolds numbers, and the results are compared with measurements, numerical simulation data, and the calculations of three different two-equation models. These comparisons show that all the models tested give essentially the same flow properties away from the wall; significant differences only occur in a region very close to the wall. In this region, the calculations of the improved k-ε model are in better agreement with measurements and numerical simulation data. In particular, the modeled distribution of the dissipation rate is significantly improved and a maximum is predicted at the wall instead of away from the wall. Furthermore, the improved k-ε model is found to be the most asymptotically consistent among the four different two-equation models examined.

I. Introduction

TURBULENCE modeling has made significant advances in the past two decades, particularly in the prediction of high-Reynolds-number flows. With the development of advanced numerical techniques, full Reynolds-stress models can now be applied with ease to calculate complex flows with and without added geometric complexity. In most calculations, the isotropic diffusivity and wall function assumptions are invoked to deal with near-wall flows. However, these assumptions are found to be less and less appropriate when improved accuracy could be achieved by applying advanced numerical techniques to solve the equations and when the complexities of the flow increase. Consequently, these simplifying assumptions have to be abandoned for the calculation of highly complex turbulent flows.[1-10] These assumptions are even more questionable when used to calculate flows with heat and mass transfer. For example, nonbuoyant heat transfer measurements[11,12] show that the streamwise heat flux is two to three times larger than the normal heat flux even under the condition of a relatively small streamwise temperature gradient. In some vertical heated pipe flow experiments, the axial heat flux was measured upward instead of downward as dictated by the eddy diffusivity assumption.[13,14] These and other reasons motivate the many contributions made to the development of low-Reynolds-number near-wall turbulence models.[1,2,6,15-17]

Although much progress has been achieved in recent years in the modeling of the Reynolds-stress and heat-flux transport equations,[15,16] the modeling of the equations that govern the transport of the dissipation rate of turbulent kinetic energy and temperature variance, on the other hand, is still rather primitive. The reason is that the exact equations are very complicated and involve terms that are either not known or very difficult to measure. As a result, the dissipation rate equations are usually modeled to give a viscous and a turbulent diffusion term, a mean-strain production term, and a viscous dissipation term. The models proposed for these terms, with the possible exception of viscous diffusion, are ad hoc at best. Therefore, it is not surprising that these equations do not perform well when extended to calculate near-wall flows.[2,6,15-17]

This paper makes an attempt to model the dissipation rate equation in the near-wall region while delaying the study of the modeling of the dissipation rate of the temperature variance equation to a later report. In the following section, the near-wall behavior of existing dissipation rate equations is first examined. A proposed improvement is then suggested. The validation of the improved dissipation rate equation is carried out using a two-equation model and the predicted near-wall behavior is compared with measurements and with direct numerical simulation (DNS) data.

II. Near-Wall Behavior of Existing Dissipation Rate Equations

According to the near-wall Reynolds-stress model of Lai and So,[15] the dissipation and velocity pressure-gradient correlation terms could be modeled to satisfy the asymptotic near-wall behavior of the exact terms in the Reynolds-stress equation. If this approach is adopted, good predictions of low-Reynolds-number plane channel flows[18,19] are obtained. The only exception is the near-wall distribution of the dissipation rate, ε. DNS data[19] show that ε reaches a plateau in the near-wall region before it increases to a maximum at the wall. The model prediction, on the other hand, gives a maximum away from the wall and a wall value that is about half that of the DNS result. When the model is applied to calculate a curved channel flow,[20] the same behavior is obtained. In spite of the discrepancy noted in the prediction of ε, the near-wall behavior of all other turbulence properties are calculated correctly, including the wall friction velocities on the convex and concave side of the channel.[17] These results seem to suggest that the prediction of ε near a wall is not affected by the modeled Reynolds-stress equation. Rather, it is influenced

Received Oct. 18, 1990; revision received April 1, 1991; accepted for publication April 8, 1991.

*Professor, Mechanical and Aerospace Engineering. Member AIAA.
†Graduate Assistant, Mechanical and Aerospace Engineering.
‡Senior Staff Scientist, ICASE. Member AIAA.

by the modeled ε equation. Further evidence in support of this conclusion can be gleaned from the heat transfer calculations of Ref. 16.

The complicated exact ε equation could be modeled to give[4]

$$C_\varepsilon = D_\varepsilon^\nu + D_\varepsilon^T + P_\varepsilon - D_\varepsilon + \xi \tag{1}$$

where the terms from left to right, respectively, represent convection, viscous diffusion, turbulent diffusion, mean-strain production, viscous dissipation of ε, and an ad hoc near-wall correction for D_ε. Various arguments[6,21,22] have been used to justify the inclusion of ξ in Eq. (1) and different approaches have been proposed for the determination of ξ. Most approaches rely on a first-order near-wall balance of the ε equation.[21,22] However, Shima[6] proposes to consider the coincidence condition

$$\frac{\partial \varepsilon}{\partial t} = \frac{\partial}{\partial t}\left(\nu \frac{\partial^2 k}{\partial x_j \partial x_j}\right) \tag{2}$$

which is guaranteed by the exact equation but not necessarily by the modeled equation. In Eq. (2), k is the turbulent kinetic energy, ν is fluid kinematic viscosity, x_j is the jth component of the spatial coordinate, and t is time. The near-wall Reynolds-stress model[15-17] adopts this idea to derive ξ. Even then, the predicted ε distribution near a wall is incorrect.

According to Mansour et al.,[23] this incorrect behavior could be traced to the models proposed for P_ε and D_ε. Their analysis shows that existing models for P_ε and D_ε, such as $P_\varepsilon = C_{\varepsilon 1}(\varepsilon/k)\tilde{P}$ and $D_\varepsilon = C_{\varepsilon 2}(\varepsilon\tilde{\varepsilon}/k)$ underpredict P_ε and D_ε in the region $0 \le y^+ < 15$. Here, $C_{\varepsilon 1}$ and $C_{\varepsilon 2}$ are model constants, $\tilde{P}$ is the production of k, $\tilde{\varepsilon} = \varepsilon - 2\nu(\partial\sqrt{k}/\partial x_j)^2$, $y^+ = yu_\tau/\nu$, u_τ is the friction velocity, and y is the normal coordinate measured from the wall. As a result, they suggest modifying P_ε and D_ε by multiplying them by f_1 and f_2, respectively. These are damping functions whose values quickly approach one for large y^+. They use DNS data to determine f_1 and f_2 and then apply the numerically determined f_1 and f_2 to P_ε and D_ε. The resultant k-ε model calculations give excellent agreement with DNS data. They also point out the importance of modeling the turbulent shear stress, $-\overline{uv}$. In general, $-\overline{uv}$ is given by

$$-\overline{uv} = \nu_t(\partial U/\partial y) = C_\mu f_\mu (k^2/\varepsilon)(\partial U/\partial y) \tag{3}$$

for simple wall shear flows, where U is the mean flow velocity, f_μ is a damping function, and C_μ is a model constant. The analysis of Ref. 23 shows that the behavior of f_μ near a wall has a significant effect on the overall calculated k and ε.

Recently, Myong and Kasagi[24] suggested that if f_μ is modeled to give a near-wall behavior of y^{-1} as compared to a conventional behavior[22,23] of y, then, only D_ε needs to be damped. In other words, f_1 can be set equal to one and they propose a new f_2 based on a form first put forward by Hanjalic and Launder.[4] Their k-ε model calculations are in good agreement with measurements. However, their calculated ε distribution near a wall is no different from those given in Refs. 6, 15–17, 21, and 22 and is contrary to that shown in Ref. 23. A variety of other two-equation models have been analyzed by Speziale et al.[25] Again, their calculated ε behavior for a boundary-layer flow is contrary to that given in Ref. 26 and is similar to those given in Refs. 6, 15–17, 21, 22, and 24. Their results are calculated based on an f_μ that behaves like y^{-1} near a wall. With the exception of ε, all other turbulence properties are predicted correctly in comparison to the data collected in Ref. 22. Once again, their results tend to show that the problem of the incorrect near-wall behavior of ε is associated with the equation for the turbulent time scale.

In the past, most of the models for f_μ gave a near-wall asymptotic behavior of y (e.g., see Ref. 22). However, this behavior is not consistent with the near-wall behavior of the turbulent shear stress. This could be easily seen by expanding the turbulent fluctuations in terms of y near a wall. If the incompressible condition is invoked, u, v, and w could be represented by the following expansions:

$$u = a_1 y + b_1 y^2 + c_1 y^3 + \cdots \tag{4a}$$

$$v = b_2 y^2 + c_2 y^3 + \cdots \tag{4b}$$

$$w = a_3 y + b_3 y^2 + c_3 y^3 + \cdots \tag{4c}$$

where a_i, b_i, and c_i are random functions of x, z, and t. Here, u, v, and w are the velocity fluctuations taken along the x, y, and z axes, respectively. Therefore, $-\overline{uv}$ varies as y^3 and k varies as y^2 near a wall. According to $\varepsilon = \nu\overline{(\partial u_i/\partial x_k)^2}$, the use of Eq. (4) results in a finite ε at the wall. Here, u_i is the ith component of the fluctuation velocity and x_k is the kth component of the coordinate. Since the behavior of U is linear in y near a wall, according to Eq. (3), f_μ has to behave like y^{-1} in order to give a y^3 behavior for $-\overline{uv}$. In other words, if the near-wall numerical simulation behavior of ε is to be properly reproduced, the asymptotic behavior of the turbulent shear stress has to be correctly modeled. This means that the suggestion of Ref. 24 and 25 for f_μ should be adopted for Eq. (3).

An attempt is now made to utilize all these findings to seek modifications to P_ε and D_ε so that the resultant ε distribution mimics DNS data[18-20,26] in the near-wall region. In this first attempt, the assumption is made that P_ε does not need correction. The only near-wall correction is to D_ε which is collected into an additional ξ function. Since the same ε equation is used for both the k-ε and Reynolds-stress models, it is prudent to start with the k-ε model. When deriving the near-wall correction for ξ, certain constraints are imposed. These are the correct behavior of $-\overline{uv}$ and f_μ in the near-wall region, the accurate predictions of k and ε as well as their limiting behavior near a wall, and an asymptotic approach of the k-ε model to its high-Reynolds-number version far away from a wall. In this way, the success of the model far away from the wall is assured. Through this analysis, it is believed that the extent of the influence of the near-wall correction on the modeled boundary-layer flow can be assessed.

III. Near-Wall Modeling of the Dissipation Rate Equation

In this investigation, stationary, two-dimensional thin shear layers or fully developed turbulent flows are considered. Therefore, only the gradient normal to the flow direction is important and the turbulent shear stress is given by $-\overline{uv}$ alone. Thus simplified, the k and ε equations become

$$\frac{\partial k}{\partial t} + U\frac{\partial k}{\partial x} + V\frac{\partial k}{\partial y} = \frac{\partial}{\partial y}\left(\nu\frac{\partial k}{\partial y}\right) + \frac{\partial}{\partial y}\left(\frac{\nu_t}{\sigma_k}\frac{\partial k}{\partial y}\right) - \overline{uv}\frac{\partial U}{\partial y} - \varepsilon \tag{5}$$

$$\frac{\partial \varepsilon}{\partial t} + U\frac{\partial \varepsilon}{\partial x} + V\frac{\partial \varepsilon}{\partial y} = \frac{\partial}{\partial y}\left(\nu\frac{\partial \varepsilon}{\partial y}\right) + \frac{\partial}{\partial y}\left(\frac{\nu_t}{\sigma_\varepsilon}\frac{\partial \varepsilon}{\partial y}\right) - C_{\varepsilon 1}\frac{\varepsilon}{k}\overline{uv}\frac{\partial U}{\partial y} - C_{\varepsilon 2}\frac{\varepsilon\tilde{\varepsilon}}{k} + \xi \tag{6}$$

where σ_k, σ_ε, $C_{\varepsilon 1}$, and $C_{\varepsilon 2}$ are model constants, U and V are the mean velocities along x and y, respectively, and ν_t is given by $C_\mu f_\mu k^2/\varepsilon$. In writing down these equations, $f_1 = f_2 = 1$ has been assumed and ξ is the only function introduced to account for wall effects. Furthermore, the dissipation term is written in terms of $\tilde{\varepsilon}$ so that it will approach a finite value at the wall. The wall boundary conditions for k and ε are given by $k_w = 0$ and $\varepsilon_w = 2\nu(\partial\sqrt{k}/\partial x_j)_w^2$ where the subscript w is used to

denote conditions at the wall. In practice, the Dirichlet boundary condition, $\varepsilon_w = 2\nu k/y^2$, could also be used provided that y is sufficiently close to the wall. It is asymptotically equivalent to the actual boundary condition, and could enhance numerical robustness of the calculations. However, in this investigation, the actual boundary condition for ε_w is used in all calculations. On the other hand, external boundary conditions depend on the type of flows considered. For boundary-layer flows, the conditions $k_\infty = 0$ and $\varepsilon_\infty = 0$ are appropriate. Here, subscript ∞ is used to denote the edge of the boundary layer. For internal flows with a symmetry axis, the conditions $\partial k/\partial\eta = 0$ and $\partial\varepsilon/\partial\eta = 0$ could be specified, where η is a coordinate normal to the symmetry axis.

The coincidence condition of Shima[6] is used to derive ξ. Based on Eq. (4) and the definition of ε, expansions for k and ε in terms of y could be derived. The result is

$$k = ay^2 + by^3 + cy^4 + 0(y^5) \tag{7a}$$

$$\varepsilon = 2a\nu + 4b\nu y + d\nu y^2 + 0(y^3) \tag{7b}$$

where a, b, c, and d are functions of x and z, and are related to the time-averaged correlations of a_i, b_i, and c_i and their derivatives. According to Shima,[6] $\partial\varepsilon/\partial t$ could be evaluated from the exact ε equation and could be shown to be given by $(-2d\nu^2 + 24c\nu^2)$ at the wall. If the suggestion of Lai and So[15] is adopted for ξ, then

$$\xi = f_{w,2}\left[-N\frac{\varepsilon\tilde{\varepsilon}}{k} + M\frac{\varepsilon^{*2}}{k}\right] \tag{8}$$

where $\varepsilon^* = \varepsilon - 2\nu k/y^2$ and N and M are to be determined, and $f_{w,2} = e^{-(R_t/64)^2}$ is a damping function introduced to ensure that ξ would vanish far away from the wall. Here, $\varepsilon^* = \varepsilon - 2\nu k/y^2$, and $R_t = k^2/\nu\varepsilon$ is the turbulent Reynolds number. Using Eqs. (4) and (7), the asymptotic behavior of the various terms in Eq. (6) could be determined. The convective terms are found to be of $0(y^2)$, while the turbulent diffusion term is deduced to be of $0(y^2)$ if ν_t is taken to be of $0(y^3)$. Similarly, the production term is estimated to be of $0(y)$. On the other hand, the remaining terms could be shown to behave as:

$$\partial[\nu\partial\varepsilon/\partial y]/\partial y = 2d\nu^2 + 0(y) \tag{9a}$$

$$\varepsilon\tilde{\varepsilon}/k = 2\nu^2(d - b^2/2a - 6c) + 0(y) \tag{9b}$$

$$\varepsilon^{*2}/k = 4b^2\nu^2/a + 0(y) \tag{9c}$$

After substituting Eq.(9) into Eq. (6) and using $(-2d\nu^2 + 24c\nu^2)$ for $\partial\varepsilon/\partial t$, the values of N and M are found to be $(2 - C_{\varepsilon 2})$ and $-1/2$, respectively.

In evaluating $\partial\varepsilon/\partial t$, Shima[6] assumed the shear flow to be essentially one-dimensional. As a result, the contributions of many terms in the exact ε equation are neglected. This means that the values of N and M thus determined are approximate at best and could be varied to give optimum predictions of near-wall flows. The ξ function as determined above is used in the near-wall k-ε model proposed in Eqs. (5) and (6) to calculate flat-plate boundary-layer flows reported in Refs. 22 and 27. In addition, Myong and Kasagi's two-equation model[24] is used to calculate the same flows so that their results could be compared with the present calculations. The set of model constants chosen are: $C_\mu = 0.096$, $C_{\varepsilon 1} = 1.5$, $C_{\varepsilon 2} = 1.83$, $\sigma_k = 0.75$, and $\sigma_\varepsilon = 1.45$. As for f_μ, the proposal of Ref. 25 is adopted, or

$$f_\mu = [1 + 3.45/\sqrt{R_t}]\tanh(y^+/115) \tag{10}$$

where the constant in f_μ is chosen to be 115 for the present investigation. It should be pointed out that the derivation of f_μ has been discussed in detail in Refs. 24 and 25. Therefore, it is not repeated here.

Preliminary calculations reveal that the results thus obtained are essentially the same for the two models examined, including the behavior of ε in the near-wall region. The present model does give a higher value for ε_w; however, the maximum ε still occurs away from the wall, rather than at the wall as indicated by DNS data.[18,26] This is believed to be a consequence of an incorrect determination of N and M. In order to optimize the values of N and M so that the calculated boundary-layer characteristics, including the near-wall behavior of ε, are fairly correct, the ξ function is rearranged to give

$$\xi = f_{w,2}\left[-2\frac{\varepsilon\tilde{\varepsilon}}{k} + (C_{\varepsilon 2}\varepsilon\tilde{\varepsilon}/\varepsilon^{*2} - 0.5)\frac{\varepsilon^{*2}}{k}\right] \tag{11}$$

Since the lowest order term of $\varepsilon\tilde{\varepsilon}/\varepsilon^{*2}$ in the near-wall region is a constant, as indicated by Eqs. (9b) and (9c), the coefficient $(C_{\varepsilon 2}\varepsilon\tilde{\varepsilon}/\varepsilon^{*2} - 0.5)$ could be replaced by a constant M_1. This new ξ function is again used to calculate the boundary-layer flows of Refs. 22 and 27. A computer optimization study reveals that the same boundary-layer properties as before are predicted if $M_1 = 1.5$ is assumed. Furthermore, with this value of M_1, the near-wall distribution of ε is found to be very similar to that given by DNS data,[18,26] namely, ε reaches its maximum value at the wall. In view of this, the ξ function given in Eq. (11) with $M_1 = 1.5$ is recommended for the improved k-ε model.

Once ξ has been determined, the ε equation could be arranged in a form similar to those of Refs. 4, 23, and 24. In other words, the terms P_ε and D_ε in Eq. (1) are multiplied by damping functions f_1 and f_2, respectively. Thus rearranged, the functions f_1 and f_2 could be deduced as $f_1 = 1$ and

$$f_2 = \left[1 + \frac{2f_{w,2}}{C_{\varepsilon 2}} - \frac{3}{2}\left(\frac{f_{w,2}}{C_{\varepsilon 2}}\right)\left(\frac{\varepsilon^{*2}}{\varepsilon\tilde{\varepsilon}}\right)\right] \tag{12}$$

This compares with $f_2 = [1 - (2/9)\exp(-R_t^2/36)][1 - \exp(-y^+/5)]^2$ proposed by Myong and Kasagi.[24] The proposal of Ref. 24 is rather empirical; however, the above approach serves to illustrate how f_2 could be derived from a consideration of the turbulence equations. It should be pointed out that the derivation is by no means unique. Furthermore, writing the ε equation in this form does not provide any real benefit to its solution. Therefore, in the following, the ε equation as given in Eq. (6) with ξ defined by Eq. (11) is used to carry out all calculations.

IV. Validation of Improved Dissipation Rate Equation

In order to validate the improved k-ε model, further comparisons are carried out with data[18,26-28] and with the calculations of three different two-equation models. One is the k-ε model given in Ref. 24, another is the k-τ model proposed in Ref. 25, while a third is the k-ω model put forward by Wilcox.[29] Only limited comparisons will be made with the k-ω model since it is not asymptotically consistent (this model was not formulated to yield accurate near-wall values for k, ε, and $-\overline{uv}$). All three models, in particular the k-ω model, have been validated against a variety of boundary-layer flows and have been found to be quite successful in their predictions of different boundary-layer characteristics. However, their predictions of the near-wall flow have not been examined in detail, in particular, the internal consistency of the models. The objectives of this validation are to assess the predictions of the near-wall flows and to examine the asymptotic consistency of the different models.

Table 1 Comparison of calculated wall properties with data for the R_θ = 1410 case

Data/Closure	$C_f \times 10^3$	a_k	$a_{uv} \times 10^4$	$k^+/\varepsilon^+ y^{+2}$
DNS–boundary layer[26]	4.10	0.130	13.0	0.50
DNS–channel flow[18]	6.04	0.083	7.2	0.50
Measurements–channel flow[28]	5.94	0.110	8.5	—
Improved k-ε	3.96	0.105	7.41	0.50
k-ε (Myong & Kasagi[24])	3.81	0.049	7.18	0.49
k-τ (Speziale et al.[25])	3.82	0.040	6.30	0.48
k-ω (Wilcox[29])	3.86	—	—	—

Near a wall, expansions (4) and (7) could be rearranged to give

$$k^+ = a_k y^{+2} + b_k y^{+3} + \ldots \tag{13a}$$

$$\varepsilon^+ = 2a_k + 4b_k y^+ + \ldots \tag{13b}$$

$$-\overline{uv}^+ = a_{uv} y^{+3} + \cdots \tag{13c}$$

where $k^+ = k/u_\tau^2$, $\varepsilon^+ = \varepsilon\nu/u_\tau^4$, $-\overline{uv}^+ = -\overline{uv}/u_\tau^2$, and the coefficients a_k, b_k, and a_{uv} are functions of x and z only. Therefore, it can be deduced that $k^+/\varepsilon^+ y^{+2}$ is exactly 0.5 at the wall and is a good measure of the asymptotic consistency of the models. Also, according to DNS data,[18,26,28] a_k varies from 0.083 to 0.13 while $a_{uv} \times 10^4$ spans a range of 7.2–13.0. These values are used to assess the accuracy of the four models examined.

Two sets of boundary-layer data are chosen for comparisons with calculations. One is the high-Reynolds-number measurements of Ref. 22 and 27 and another is the low-Reynolds-number DNS data of Ref. 26. In the measurement case, the comparisons are made at a location of $x \cong 5$ m with $R_x = 1.156 \times 10^7$ and $R_\theta = 16{,}465$, where R_x and R_θ are the Reynolds number based on x and the momentum thickness θ, respectively. Three cases at different R_θ ranging from 300 to 1410 are presented in Ref. 26. A detailed comparison of the $R_\theta = 1410$ case is carried out because k budget data is also available for this case. In this way, the ability of the different models to predict near-wall flows over a wide range of R_θ can be assessed.

The first comparison is carried out with the DNS data of Spalart.[26] Four different two-equation models are used to calculate the case where $R_\theta = 1410$. Comparisons shown in Figs. 1–4 are made with the distributions of u^+, k^+, ε^+, and $-\overline{uv}^+$ vs y^+, while the limiting values of k^+, ε^+, and $-\overline{uv}^+$ are tabulated in Table 1. It should be pointed out that the k-ω model is not consistent asymptotically, therefore, its limiting values are not listed in the table. As far as near-wall flows are concerned, they are similar for internal as well as for external flows. Therefore, the channel flow data of Refs. 18 and 28 are also included in Table 1 for comparison. The data from Ref. 18 are obtained from direct numerical simulation at $R_D = 6500$, where R_D is the Reynolds number based on channel width and centerline velocity. On the other hand, the measurements of Ref. 28 are obtained at $R_D = 7510$. Since ε is not reported in Ref. 28, $k^+/\varepsilon^+ y^{+2}$ could not be determined. From this tabulation, it can be seen that there are great differences between the values reported for a_k and a_{uv} (Table 1). Also, C_f for the boundary-layer flow is substantially lower than the channel flow values. The reason is the corresponding R_θ for the channel flow is lower than that of the boundary-layer flow. Therefore, when comparing calculations with channel flow data, a C_f comparison should be avoided. The comparison should be carried out with the asymptotic behavior of the turbulence characteristics only, because these values are relatively independent of Reynolds number.

Predictions of the mean velocity field by the four different two-equation models are essentially similar. This means that the mean velocity distribution is not too sensitive to the proposed near-wall correction (Fig. 1). As a result, the u^+ vs y^+ plots for the four models listed in Table 1 are essentially identical and the log region can be described by

$$u^+ = \frac{1}{\kappa} \ln y^+ + B \tag{14}$$

where the von Karman constant, κ, is determined to be 0.35 and smaller than $\kappa = 0.41$ given by DNS data (Fig. 1). In other words, all two-equation models predict an earlier departure from true behavior as the Reynolds number is decreased. The constant B is calculated to be 4.4 and is substantially smaller than the DNS value of 5.0. This essentially is a consequence of the difference in κ. The distributions of k^+, ε^+, and $-\overline{uv}^+$ away from the wall are practically identical for the four models studied. Therefore, they are not shown here. However, there are substantial differences in the near-wall region (Figs. 2–4). First, the predicted a_k is largest for the improved k-ε model and smallest for the other models (Table 1). According to DNS data, $a_k = 0.13$. The present prediction gives a value of 0.105. Even though this value is not quite correct compared to the DNS data of Refs. 18 and 26, it is in agreement with the channel flow measurement of Ref. 28. As for the other models, their predictions of a_k are substantially lower than the data collected in Table 1. Second, the calculated k^+ distribution from the improved k-ε model is only slightly higher than the DNS result: however, the other calculated distributions are lower than the DNS data (Fig. 2). It can be seen that the lowest maximum k^+ value is given by the k-τ model. Third, with the exception of the improved k-ε model, all models examined give an ε^+ distribution that reaches a maximum away from the wall and then drops to a finite value at the wall (Fig. 3.). In the case of the k-ω model, the wall value of ε^+ is very close to zero. On the other hand, the present prediction of ε^+ gives a plateau at about the same location where the other models produce a maximum. There-

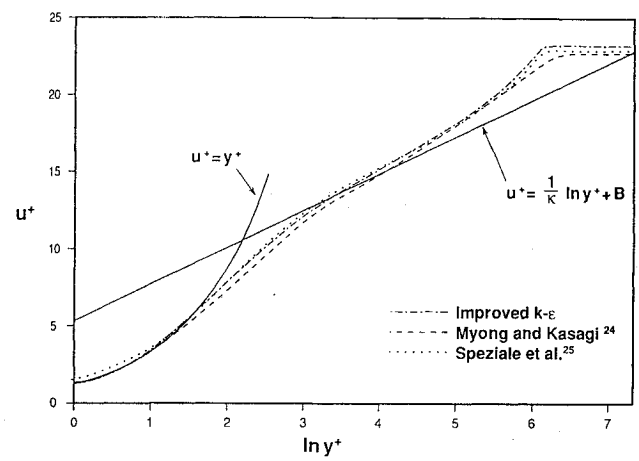

Fig. 1 Calculated mean velocities in semilog plot (R_θ = 1410).

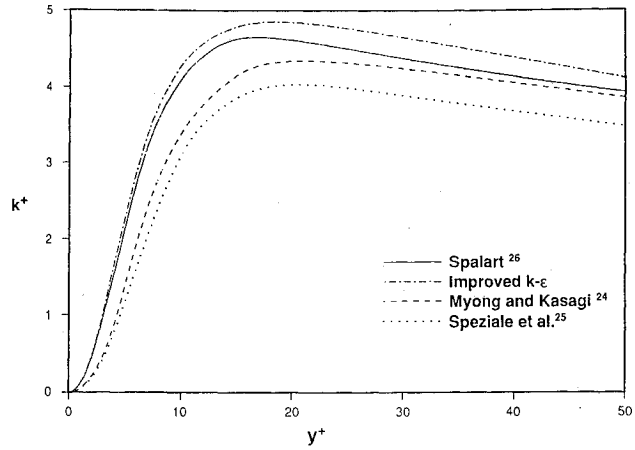

Fig. 2 Comparison of the calculated k in the near-wall region (R_θ = 1410).

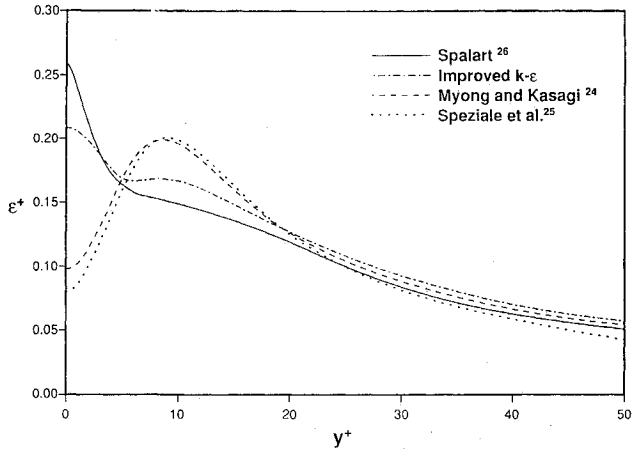

Fig. 3 Comparison of the calculated ε in the near-wall region (R_θ = 1410).

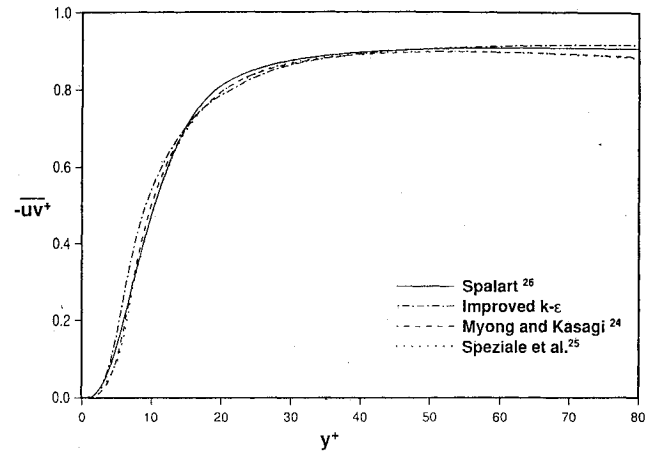

Fig. 4 Comparison of the calculated shear stress in the near-wall region (R_θ = 1410).

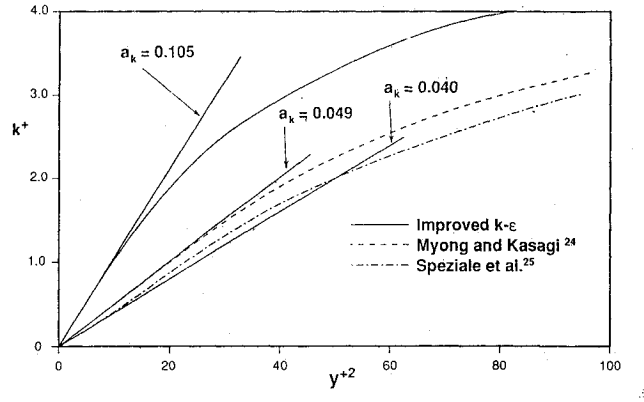

Fig. 5 Asymptotic behavior of k^+ (R_θ = 1410).

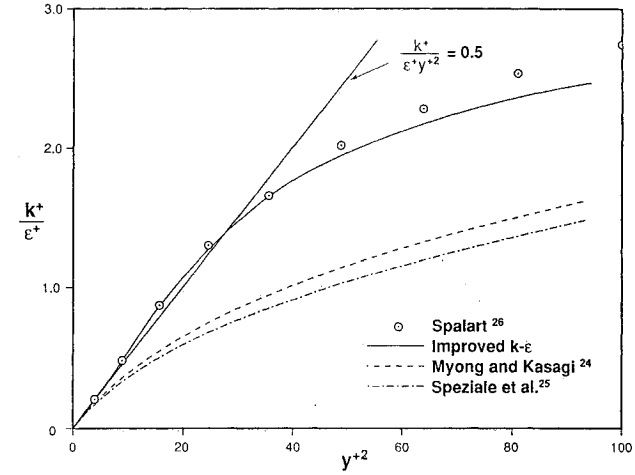

Fig. 6 Asymptotic behavior of k^+/ε^+ (R_θ = 1410).

after, ε^+ increases to a maximum at the wall. A comparison of this behavior with DNS data[26] reveals that the near-wall behavior of ε^+ is similar to that given by DNS; however, the present prediction is lower than the calculation of Ref. 26. It should be noted that when compared with the data of Ref. 18, the present near-wall ε^+ prediction is higher than the channel flow calculation. In spite of this discrepancy, the prediction of the k budget is in excellent agreement with DNS data.[26] More will be said about this later when the k budgets are compared. Finally, the near-wall comparison of $-\overline{uv}^+$ is shown in Fig. 4. All model calculations are similar and in fairly good agreement with DNS data.

The limiting wall values and C_f are listed in Table 1. In the case of C_f, all model predictions are similar and in good agreement with DNS data. On the other hand, the prediction of $k^+/\varepsilon^+ y^{+2}$ varies from 0.48 to 0.5. The correct value is given by the improved k-ε model. As pointed out above, the improved k-ε model gives the most correct prediction of a_k and hence ε_w. The other model calculations are substantially lower than the DNS data. Since the prediction of u^+ by all models examined are essentially identical, the predicted values of a_{uv} do not vary widely like those of a_k. The calculated a_{uv} are low compared to the DNS data of Ref. 26, however, they are in good agreement with the values of Refs. 18 and 28. In summary, it could be said that the improved k-ε model gives a correct and internally consistent prediction of the near-wall flow in flat-plate boundary layers.

Further evidence in support of this conclusion can be gleaned from the asymptotic plots of k^+ vs y^{+2}, k^+/ε^+ vs y^{+2}, and $-\overline{uv}^+$ vs y^{+3}. These are given in Figs. 5–7. The k-ω results are not plotted for reasons stated above, while the inferred result of k^+/ε^+ from Ref. 26 is also shown in Fig. 6 for comparison. According to Fig. 5, the range in which the slope of k^+ vs y^{+2} remains constant is about $0 \le y^+ \le 5$ for the k-ε[24] and k-τ[25] models and about $0 \le y^+ \le 4$ for the improved k-ε model. However, it should be noted that both the slope and the distribution of k^+ within the range $0 \le y^+ \le 10$ is essentially independent of R_θ for the improved k-ε model but not so for the other models. This can be seen from the calculated a_k for the high R_θ case (Table 2). Furthermore, when the k^+ vs y^{+2} curves for the high R_θ case are plotted in Fig. 5, the improved k-ε model curve coincides with the present one

Table 2 Comparison of calculated wall properties with data for the R_θ = 16,465 case

Data/Closure	$C_f \times 10^3$	a_k	$a_{uv} \times 10^4$	$k^+/\varepsilon^+ y^{+2}$
Data of Weighardt and Tillman[27] and Patel et al.[22]	2.43	0.025 to 0.05	—	—
Improved k-ε	2.47	0.107	7.32	0.50
k-ε (Myong & Kasagi[24])	2.46	0.054	7.54	0.49
k-τ (Speziale et al.[25])	2.44	0.044	6.7	0.49
k-ω (Wilcox[29])	2.44	—	—	—

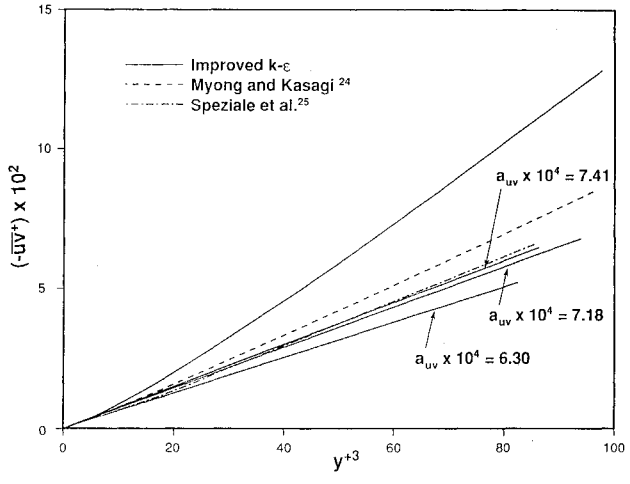

Fig. 7 Asymptotic behavior of $-uv^+$ (R_θ = 1410).

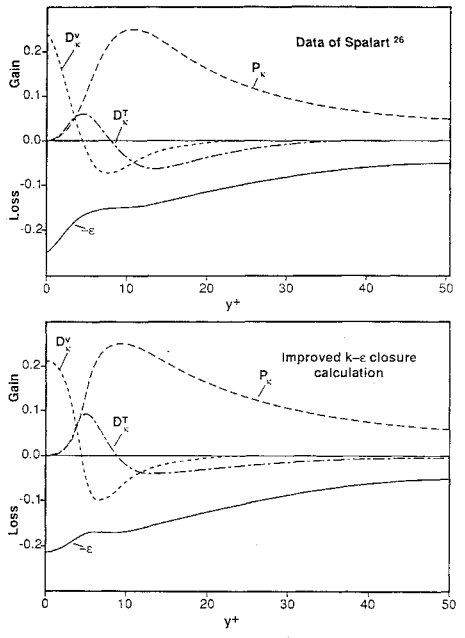

Fig. 8 The budget of k in the near-wall region (R_θ = 1410).

while other model calculations show a deviation as early as $y^+ = 2$. In order to avoid clutter, these high R_θ curves are not shown in Fig. 5. The same is also true of the distributions given in Figs. 6 and 7. This Reynolds number independence behavior of the present model is consistent with DNS data[26] and suggests that essential near-wall physics has been properly accounted for in the present model. Other two-equation models are Reynolds number dependent in the near-wall region and, thus, fail to capture near-wall physics properly. The most convincing evidence that the improved k-ε model is more correct in the near-wall region and asymptotically consistent is illustrated in Fig. 6. In this plot, it can be seen that the present prediction of k^+/ε^+ is in excellent agreement with DNS data up to $y^+ = 7$. However, other model calculations are substantially lower than DNS data and the deviation starts as early as $y^+ = 1$. Finally, the slope of $-\overline{uv}^+$ vs y^{+3} remains constant up to $y^+ = 4$ for the improved k-ε model and to about $y^+ = 3$ for the other models (Fig. 7).

The improved k-ε model calculation of the k budget in the near-wall region is shown in Fig. 8 for comparison with DNS data.[26] Other results are not shown because their predictions of ε in the near-wall region are incorrect, both qualitatively and quantitatively. In this figure, only the viscous (D_k^ν) and turbulent (D_k^T) diffusion of k, the production (P_k) of k, and the dissipation ($-\varepsilon$) of k are plotted. Since the convection of k is approximately zero in the near-wall region, it is not shown in Fig. 8. At the wall, viscous diffusion balances dissipation. This balance extends to about $y^+ = 2$. In the region, $2 \leq y^+ < 15$, all four terms are of equal importance. Beyond $y^+ = 15$, the turbulence is in local equilibrium, that is, production of k balances the dissipation of k. A maximum P_k of 0.25 is predicted at $y^+ = 9.4$, which compares favorably with DNS data of 0.246 at $y^+ = 10.4$. The distribution of D_k^ν is equally well predicted as evidence by the calculated minimum of $D_k^\nu = -0.1$ at $y^+ = 7.0$ compared to DNS data of $D_k^\nu = -0.075$ at $y^+ = 7.5$. Even though gradient transport is assumed for turbulent diffusion, the model calculation of D_k^T is in good agreement with data. The maximum is predicted to be 0.091 at $y^+ = 5.0$. This compares with DNS data of 0.06 at the same y^+. Therefore, it can be said, with the exception of the quantitative near-wall prediction of ε, the budget of k is in excellent agreement with DNS data. This comparison further shows that the equilibrium turbulence assumption is applicable for $y^+ \geq 15$ and is consistent with DNS data.[18,26]

The high R_θ case is presented next. Plots of the mean velocity in terms of u^+ vs $\ell n y^+$ are shown in Fig. 9, while the near-wall plots of k^+, ε^+, and $-\overline{uv}^+$ vs y^+ are given in Figs. 10–12. The calculated values at the wall including the skin friction coefficient C_f are listed in Table 2. Even though the measured a_k are also listed, it should be noted that they are substantially lower than the values quoted in Refs. 18, 26, and 28. The values quoted in Table 2 were not obtained using state-of-the-art diagnostic techniques, therefore, they were subjected to large measurement errors[28] and are not to be trusted in a strict sense. Such sentiments have also been expressed by the investigators of the experimental work collected in Ref. 22. In view of this, a comparison of a_k with measurements should be made with caution.

The following conclusions can be drawn from these comparisons. First and foremost, the mean velocity distribution is not too sensitive to the proposed near-wall correction (Fig. 9). As a result, the u^+ vs $\ell n y^+$ plots for the four models listed in Table 2 are essentially identical and the log region can again be described by Eq. (14). In this case, κ is determined to be 0.41, and the constant B is found to be about 5.0. These values of κ and B are in excellent agreement with measurements. Second, the distributions of k^+, ε^+, and $-\overline{uv}^+$ beyond $y^+ = 100$ are essentially the same; thus, indicating that the near-wall correction to D_ε has little or no effect on the behavior of k^+, ε^+, and $-\overline{uv}^+$ beyond $y^+ = 100$ (Figs. 10–12). However, it does affect the predicted maximum values of k^+

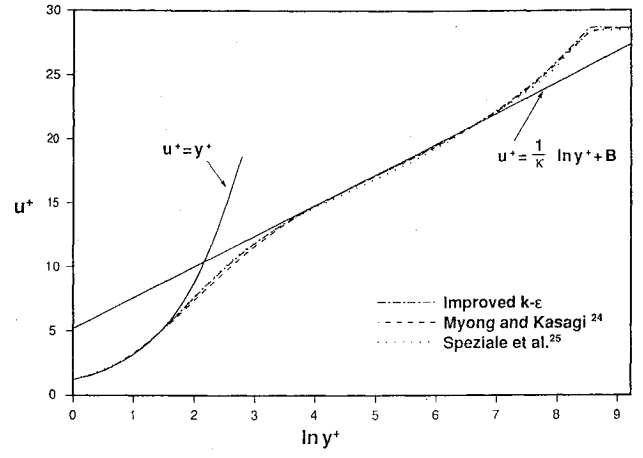

Fig. 9 Calculated mean velocities in semilog plot (R_θ = 16,465).

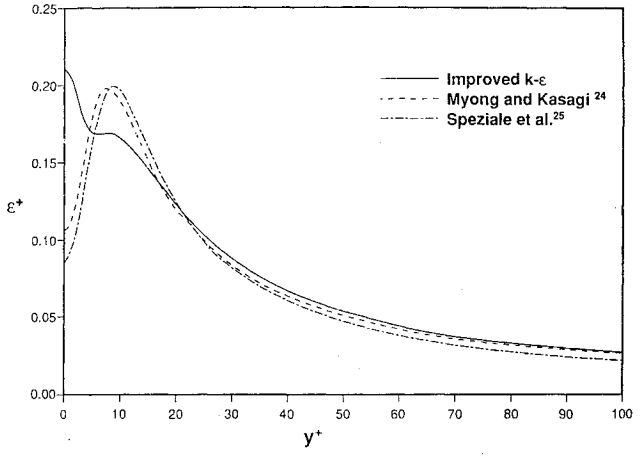

Fig. 11 Comparison of the calculated ε in the near-wall region (R_θ = 16,465).

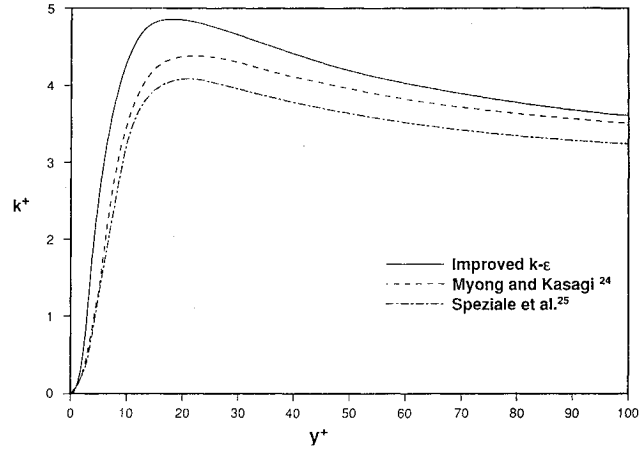

Fig. 10 Comparison of the calculated k in the near-wall region (R_θ = 16,465).

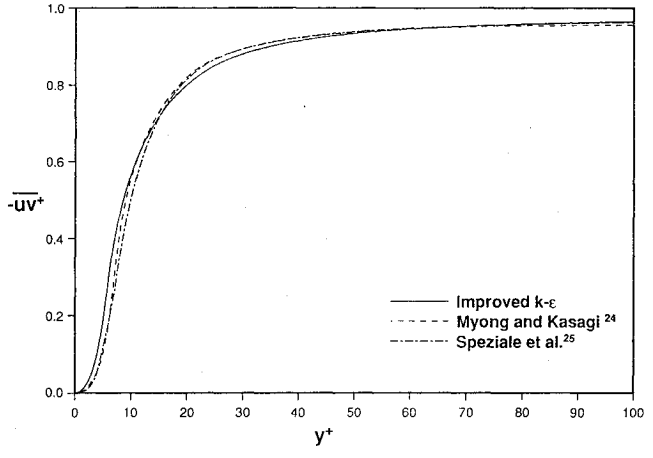

Fig. 12 Comparison of the calculated shear stress in the near-wall region (R_θ = 16,465).

and ε^+. Even though the maximum k^+ calculated by the improved k-ε model is the highest among the four models compared, it is consistent with the mean curve drawn through all the data collected in Ref. 22. Third, the near-wall correction significantly affects the behavior of ε^+ (Fig. 11) but much less so the behavior of k^+ and $-\overline{uv}^+$ (Figs. 10 and 12) in the region $0 \le y^+ < 20$. Fourth, the value of a_k and hence $\varepsilon_w^+ = 2a_k$ is very much affected by the proposed near-wall correction (see Table 2). The improved k-ε model gives a value of a_k that is more consistent with DNS data and substantially higher than measurements. On the other hand, there is not much difference in the calculated a_{uv} and the near-wall distributions of $-\overline{uv}^+$ are essentially the same for the three model calculations shown in Fig. 12. Fifth, the calculated $k^+/\varepsilon^+ y^{+2}$ is exactly 0.5 for the improved k-ε model and suggests that it is the most internally consistent model among the four examined (see Table 2). Finally, the near-wall distribution of ε^+ is very much influenced by the proposed near-wall correction. The present improvement gives a maximum ε^+ at the wall while the others give a maximum ε^+ away from the wall (Fig. 11). Furthermore, the models of Refs. 24, 25, and 29 predict the location where the maximum ε^+ occurs to be at about $y^+ = 10$, which is approximately coincident with the location of the ε^+ plateau in the present calculation (Fig. 11).

V. Conclusions

The near-wall behavior of several modeled ε equations has been examined. It is found that all equations studied give fairly good predictions of ε^+ down to $y^+ = 30$. However, their calculations of ε^+ in the region $0 \le y^+ \le 30$ are incorrect, both qualitatively and quantitatively. The cause of this discrepancy is traced to the ε equation, in particular, the incorrect near-wall behavior of the models proposed for the dissipation term in the equation. Various near-wall corrections have been proposed for the dissipation term, however, none gives a satisfactory prediction of ε^+ in the near-wall region. In this study, a new near-wall correction for the dissipation term in the ε equation has been proposed. It is derived using the concept of near-wall coincidence of ε proposed by Shima.[6] Two model constants are introduced. One could be determined exactly by applying the coincidence condition, while the other constant is determined by requiring the near-wall behavior of ε^+ to mimic DNS data.

The improved k-ε model is then used to calculate flat-plate boundary-layer flows that span a large range of R_θ. Calculated results are compared with measurements, DNS data, and the predictions of three different two-equation models. The comparisons show that the predictions of all four models are very similar far away from the wall and in good agreement with measurements and DNS data. In the near-wall region, the predictions, in particular those of ε^+, disagree with each other and with DNS data. Only the improved k-ε model is capable of predicting the near-wall behavior of ε^+ correctly from a qualitative standpoint. That is, ε^+ is calculated to reach its maximum at the wall rather than away from the wall. All other models studied give a maximum away from the wall. The improved k-ε model overestimates the maximum k^+ slightly, while other models underpredict the maximum k^+ substantially. Another feature of the improved k-ε model is

that its predicted near-wall properties are Reynolds number independent while other model calculations are not. The near-wall Reynolds number independence character is consistent with DNS data. Furthermore, the present prediction of $k^+/\varepsilon^+ y^{+2}$ is exactly equal to 0.5 and its distribution is in excellent agreement with DNS data up to $y^+ = 7$. Therefore, this suggests that the improved k-ε model is internally more consistent than other two-equation models examined.

Acknowledgments

Funding support for the first and second authors under Grant NAG-1-1080 from NASA Langley Research Center, is gratefully acknowledged. The grant is monitored by T. B. Gatski. The third author acknowledges the support of NASA under Contract NAS1-18605 while in residence at ICASE.

References

[1]Rodi, W., "Recent Developments in Turbulence Modeling," *Proceeding of the 3rd International Symposium on Refined Flow Modeling and Turbulence Measurements*, Tokyo, July 26–28, 1988, pp. 1–15.

[2]Launder, B. E., and Tselepidakis, D.P., "Contribution to the Second-Moment Modeling of Sublayer Turbulent Transport," *Proceeding of the Zaric Memorial International Seminar on Wall Turbulence*, Dubrovnik, Yugoslavia, 1988, pp. 1–16.

[3]Cousteix, J., "Three-Dimensional and Unsteady Boundary Layer Computation," *Annual Review of Fluid Mechanics*, Vol.18, 1986, pp. 173–196.

[4]Hanjalic, K., and Launder, B. E., "Contribution Towards a Reynolds-Stress Model for Low-Reynolds-Number Turbulence," *Journal of Fluid Mechanics*, Vol. 74, 1976, pp. 593–610.

[5]So, R. M. C., and Yoo, G. J., "Low-Reynolds-Number Modelling of Turbulent Flows With and Without Wall Transpiration," *AIAA Journal*, Vol. 25, 1987, pp. 1556–1564.

[6]Shima, N., "A Reynolds-Stress Model for Near-Wall and Low-Reynolds-Number Regions," *Journal of Fluids Engineering*, Vol. 110, 1988, pp. 38–44.

[7]Yoo, G. J., and So, R. M. C., "Variable Density Effects on Axisymmetric Sudden-Expansion Flows," *International Journal of Heat and Mass Transfer*, Vol. 32, 1989, pp. 105–120.

[8]Launder, B. E., "On the Computation of Convective Heat Transfer in Complex Turbulent Flows," *Journal of Heat Transfer*, Vol. 110, 1988, pp. 1112–1128.

[9]Launder, B. E., "Numerical Computation of Convective Heat Transfer in Complex Turbulent Flows: Time to Abandon Wall Functions?" *International Journal of Heat and Mass Transfer*, Vol. 27, 1984, pp. 1485–1491.

[10]So, R. M. C., Lai, Y. G., Hwang, B. C., and Yoo, G. J., "Low-Reynolds-Number Modelling of Flows over a Backward-Facing Step," *Zeitschrift fur angewandte Mathematik und Physik*, Vol. 39, 1988, pp. 13–27.

[11]Bremhorst, K., and Bullock, K. J., "Spectral Measurements of Temperature and Longitudinal Velocity Fluctuations in Fully Developed Pipe Flow," *International Journal of Heat and Mass Transfer*, Vol. 13, 1970, pp. 1313–1329.

[12]Bremhorst, K., and Bullock, K. J., "Spectral Measurement of Turbulent Heat and Momentum Transfer in Fully Developed Pipe Flow," *International Journal of Heat and Mass Transfer*, Vol. 16, 1973, pp. 2141–2154.

[13]Carr, A. D., Connor, M. A., and Buhr, H. O., "Velocity, Temperature and Turbulence Measurements in Air for Pipe Flow with Combined Free and Forced Convection," *Journal of Heat Transfer*, Vol. 95, 1973, pp. 445–452.

[14]Hochriter, L. E., and Sesonske, A., "Turbulent Structure of Isothermal and Non-isothermal Liquid Metal Pipe Flow," *International Journal of Heat and Mass Transfer*, Vol. 17, 1974, pp. 113–128.

[15]Lai, Y. G., and So, R. M. C., "On Near-Wall Turbulent Flow Modelling," *Journal of Fluid Mechanics*, Vol. 221, 1990, pp. 641–673.

[16]Lai, Y. G., and So, R. M. C., "Near-Wall Modelling of Turbulent Heat Fluxes," *International Journal of Heat and Mass Transfer*, Vol. 33, 1990, pp. 1429–1440.

[17]So, R. M. C., Lai, Y. G., and Hwang, B. C., "Near-Wall Turbulence Model for Curved Flows," *AIAA Journal*, Vol. 29, 1991, 1202–1214.

[18]Kim, J., Moin, P., and Moser, R., "Turbulence Statistics in Fully Developed Channel Flow at Low Reynolds Number," *Journal of Fluid Mechanics*, Vol. 177, 1987, pp. 133–166.

[19]Mansour, N. N., Kim, J., and Moin, P., "Reynolds-Stress and Dissipation-Rate Budgets in a Turbulent Channel Flow," *Journal of Fluid Mechanics*, Vol. 194, 1988, pp. 15–44.

[20]Moser, R. D., and Moin, P., "The Effects of Curvature in Wall-Bounded Turbulent Flows," *Journal of Fluid Mechanics*, Vol. 175, 1987, pp. 479–510.

[21]Chien, K. Y., "Predictions of Channel and Boundary-Layer Flows with a Low-Reynolds-Number Two-Equation Model of Turbulence," *AIAA Journal*, Vol. 20, 1982, pp. 33–38.

[22]Patel, V. C., Rodi, W., and Scheuerer, G., "Turbulence Models for Near-Wall and Low-Reynolds-Number Flows: A Review," *AIAA Journal*, Vol. 23, 1985, pp. 1308–1319.

[23]Mansour, N. N., Kim, J., and Moin, P., "Near-Wall k-ε Turbulence Modeling," *AIAA Journal*, Vol. 27, 1989, pp. 1068–1073.

[24]Myong, H. K., and Kasagi, N., "A New Approach to the Improvement of k-ε Turbulence Model for Wall Bounded Shear Flows," *JSME International Journal*, Series II, Vol. 33, 1990, pp. 63–72.

[25]Speziale, C. G., Abid, R., and Anderson, E. C., "A Critical Evaluation of Two-Equation Models for Near Wall Turbulence," AIAA Paper 90-1481, 1990.

[26]Spalart, P. R., "Direct Simulation of a Turbulent Boundary Layer up to $R_\theta = 1410$," *Journal of Fluid Mechanics*, Vol. 187, 1988, pp. 61–98.

[27]Wieghardt, K., and Tillmann, W., "On the Turbulent Friction Layer for Rising Pressure," NACA TM-1314, 1951.

[28]Nishino, K., and Kasagi, N., "Turbulence Statistics Measurement in a Two-Dimensional Channel Flow Using a Three-Dimensional Particle Tracking Velocimeter," *Seventh Symposium on Turbulent Shear Flows*, Stanford Univ., Stanford, CA, Aug. 21–23, 1989, pp. 22.1.1–22.1.6.

[29]Wilcox, D. C., "Reassessment of the Scale-Determining Equation for Advanced Turbulence Models," *AIAA Journal*, Vol. 26, 1988, pp. 1299–1310.